Minimization of Recombinant Human Flt3 Ligand Aggregation at the T_m Plateau: A Matter of Thermal Reversibility

Richard L. Remmele, Jr.,*,‡ Saraswaty D. Bhat,§ Duke H. Phan,‡ and Wayne R. Gombotz‡

Analytical Chemistry and Formulation, Immunex Corporation, Seattle, Washington 98101, and Analytical Development and Quality Control, Biogen, Cambridge, Massachusetts 02142

Received December 7, 1998; Revised Manuscript Received February 23, 1999

ABSTRACT: This study elucidates the importance of thermal reversibility as it pertains to the minimization of recombinant human Flt3 ligand aggregation and its potential role for determining solution conditions that can achieve the greatest long-term storage stability. Both thermal reversibility and T_m were evaluated as microcalorimetric parameters of stability within the range extending from pH 6 to 9, where the T_m was shown to plateau near 80 °C. Within this region, the reversibility was shown to decrease from 96.6% to 15.2% while the pH was increased from 6 to 9, respectively. Accelerated stability studies conducted at 50 °C exhibited rates of aggregation augmented by pH that inversely correlated with the thermal reversibility data. Namely, high thermal reversibility at the T_m plateau correlated with slower rates of aggregation. Enthalpic calorimetric to van't Hoff ratios ($\Delta H_1/\Delta H_v$) yielded results close to unity within the plateau region, suggesting that the unfolding of rhFlt3 ligand was approximately two-state. Evidence that unfolding preceded the formation of the aggregate was provided by far-UV CD data of a soluble islolate of the aggregated product exhibiting a 28% loss of α-helix offset by a 31% gain in β-sheet. This information combined with the thermal reversibility data provided compelling evidence that unfolding was a key event in the aggregation pathway at 50 °C. Minimization of aggregation was achieved at pH 6 and corroborated by evidence acquired from sodium dodecyl sulfate−polyacrylamide gel electrophoresis and size exclusion data. Correspondingly, the bioactivity was found to be optimal at pH 6. The findings link thermal reversibility to the propensity of Flt3 ligand to aggregate once unfolded in the T_m plateau region and provide a basis for relating the reversibility of thermal denaturation to the prediction of long-term storage stability in aqueous solution.

Changes in the melting transition temperature (T_m),[1] or denaturation temperature of unfolding as it is sometimes called, can be a measure of a solution's influence on the stability of a protein (*1*−*3*). The T_m is related to the change in free energy between the native and denatured states of a protein molecule (i.e., Gibbs−Helmholtz equation) and, therefore, is a thermodynamic parameter of conformational stability (*2*, *4*). An important condition of thermodynamic modeling involves the equilibrium between these states, which can be measured experimentally in a differential scanning calorimeter (DSC). This equilibrium is essentially equivalent to the reversibility of the enthalpy accompanying the melting transition between the folded and unfolded states. Although reversibility is a requirement for thermodynamic characterization of a given protein system, little attention has been given to the role it might play as a parameter of irreversible denaturation and its implications as a measure of protein stability in aqueous solutions. Irreversibility can be viewed as a competing pathway of the equilibrium between the native and unfolded states. Irreversible unfolding events include aggregation (i.e., intermolecular disulfide cross-linking, hydrophobic self-association) and nonnative refolding (perhaps due in part to chemical modification or incomplete refolding from the unfolded state).

Problems can arise that make it difficult to thermodynamically characterize some protein systems. Many aqueous protein systems yield little or no reversibility (*5*, *6*). Under these conditions an initial scan in the calorimeter may only permit determination of the T_m. Additionally, an exothermic event originating from aggregation can obscure T_m measurements, especially if they occur at or near the T_m (*7*, *8*). To address the role of reversibility independent of T_m, a protein system should ideally exhibit thermal reversibility that is responsive to changing conditions of a given solution environment where the T_m is least affected (i.e., remains constant and is essentially free of exothermic obscurities).

Flt3 ligand is a protein system possessing such behavior when solution pH conditions are varied between pH 6 and 9. This protein is a member of a family of growth factors that stimulate the proliferation of hematopoietic cells (*9*). It consists of 153 amino acids with an average polypeptide molecular mass of 17.4 kDa and a p*I* ranging from 3.8 to 5.2 (due to differently glycosylated isoforms of the molecule). It structurally belongs to the short-chain helical bundle family

* To whom correspondence should be addressed: Immunex Corp., 51 University St., Seattle, WA 98101. Phone 206-587-0430, ext. 4418; FAX 206-233-9733; E-mail rremmele@immunex.com.

‡ Immunex Corp.

§ Biogen.

[1] Abbreviations: CCA, convex constraint analysis; DSC, differential scanning calorimetry; rhFlt3L, recombinant human Flt3 ligand; SDS−PAGE, sodium dodecyl sulfate−polyacrylamide gel electrophoresis; SEC, size exclusion chromatography; T_m, melting transition temperature.

10.1021/bi982881g CCC: $18.00
Published on Web 04/02/1999

of cytokines that includes macrophage colony stimulating factor (M-CSF) (*9*−*11*). This study investigates the role of T_m and thermal reversibility in delineating solution conditions that confer minimal aggregation and the implications related to storage stability.

MATERIALS AND METHODS

Materials. Recombinant human Flt3L was obtained as a purified bulk drug concentrate prepared at Immunex. It was dialyzed against a polybuffer system and diluted with either acid (HCl) or base (NaOH) to achieve the desired pH before reaching a final concentration near 5 mg/mL. The polybuffer system used in the DSC measurements consisted of 50 mM sodium citrate (J. T. Baker), 20 mM NaCl (J. T. Baker), 20 mM KH_2PO_4 (Mallinckrodt), 17 mM L-arginine (EM Science), 40 mM L-glycine (J. T. Baker), 25 mM HEPPS (Sigma), and 20 mM HEPES (J. T. Baker). Use of this system was intended to normalize the influence of the buffering components and permit an assessment of pH on the thermal unfolding transition.

Differential Scanning Calorimetric Studies. The solutions containing 5 mg/mL protein were subjected to DSC analysis with a microcalorimeter (MicroCal MC-2, MicroCal). The scan rate in each case was 68 °C/h. The thermograms were background-corrected and rescans were employed to evaluate the reversibility of the unfolding transition at desired pH. The extent of reversibility was measured by dividing the enthalpy recovered on the second upscan (designated ΔH_2) by the same of the first upscan ($\Delta H_1 = \Delta H_{cal}$) reported as a percent

$$\% \text{ reversibility} = \Delta H_2/\Delta H_1(100) \quad (1)$$

In this study 90 °C was set as the upper temperature limit, which was well beyond the completion of the T_m of rhFlt3L. The T_m values for transitions on the second scan were identical to those on the first. All data manipulation was performed with the Origin software provided with the instrument.

Stability Studies. Accelerated stability studies were carried out with solutions consisting of 1 mg/mL rhFlt3L incubated at 50 °C. One-milliliter volumes, appropriately buffered, were placed within 2 mL type I glass vials under aseptic conditions. The vials were then subsequently stoppered, capped, and crimped. Two vials per formulation condition were prepared and incubated for either 2 weeks or 1 month. The buffering systems used included sodium citrate (pH 6.1), sodium phosphate (pH 7.0, 8.0, and 9.1), and a control (freshly thawed protein after storage at −70 °C at pH 7.4).

Sodium Dodecyl Sulfate−*Polyacrylamide Gel Electrophoresis.* Nonreduced SDS−PAGE silver-stained gels were prepared to qualitatively assess stability (i.e., breakdown, aggregation). A 5 μg protein load/well was run on a Novex 10−27% Tris−glycine gradient gel. Gels were run with a current of 20−25 mA until the dye front reached the gel foot. The gel was subsequently stained with 1 mL of 19.4% silver nitrate/100 mL of silver staining solution and then developed for visualization of the protein-banding pattern.

Size Exclusion Chromatography. A Bio-Sil 125 column was used with a Waters HPLC system to quantitatively evaluate aggregation and/or breakdown products. A flow rate of 1 mL/min with phosphate-buffered saline (PBS) (pH 7) as the elution buffer permitted adequate separation of the aggregation products when 20 μg of protein was injected onto the column in a 20 μL sample volume. Detection of eluting components was measured at 220 nm (Waters 996 photodiode array detector). Aggregate and native (nondegraded protein) compositions were determined as a percent area of high molecular weight species (eluting between 5 and 6 min) and the main peak (eluting between 6 and 9 min), respectively. Integration was carried out from the elution baseline.

Three-Detector Light Scattering Assessment of Molecular Weight. The oligomerization of rhFlt3L in solution (in its native form) was investigated by the SEC−UV/LS/RI method (on-line SEC followed by ultraviolet detection at 280 nm, light scattering at 90° (LS), and refractive index (RI) detectors in tandem). Details of the flow cell used in the light scattering detection measurements have already been published (*12*). The "three detector" technique offers the advantage of assessing the nonglycosylated polypeptide molecular weight of glycosylated proteins (*13*−*15*). Light scattering and refractive index measurements were collected with a DAWN DSP and Optilab differential refractometer (products of Wyatt Technology Corporation). Experiments were carried out on an Integral HPLC system (PerSeptive Biosystems, Inc.) with a Superdex 200 HR 10/30 column (Pharmacia Biotech). Column load was 200 μg/run. Elution conditions included a flow rate of 1 mL/min with a 200 mM sodium phosphate mobile phase at pH 8. All detector systems were calibrated with ovalbumin (Sigma), bovine serum albumin monomer (Sigma), and bovine serum albumin dimer (Sigma) at a nominal concentration of 1 mg/mL in each case (*13*−*15*). The resulting plot of $(LS)(UV)/[\epsilon(RI)^2]$ as a function of molecular weight was linear, passing through the origin and having a $r^2 = 0.994$. The slope of this plot provided the combined instrumental calibration constant k'' (147.037) used in the determination of the molecular weight of rhFlt3L in aqueous solution. The experimental molar extinction coefficient (ϵ) used in the assessment was found to be 1.63. Data were acquired with ASTRA (version 4.2, Wyatt Technology Corp.).

Isolation of Pure Aggregate Species. For the isolation of the rhFlt3L aggregate species, a Bio-Sil SEC 400-5 column was used to allow for greater resolution of the aggregate than was possible with the Superdex 200 or the Bio-Sil 125. Elution conditions in this case were 1 mL/min flow rate, 200 mM sodium phosphate elution buffer (pH 7.2), and approximately a 200 μg injection load. Fractions were subsequently collected in the region extending from the exclusion limit (4.8 min) to approximately 7 min and pooled to yield the isolated aggregate species. Solutions were consequently reexamined to ensure that the islolate was free of any native species. Once assured of pure isolation of the aggregate form, the sample was buffer exchanged into 25 mM sodium phosphate (pH 7) and concentrated to 225 μg/mL to be examined by CD.

Circular Dichroism. Far-UV CD examination of the native and aggregate forms was carried out using a J-600 spectropolarimeter (Jasco, Inc.). Prior to analyzing the sample, the instrument was calibrated with ammonium d-10-camphorsulfonic acid. Both protein forms were evaluated in 25 mM sodium phosphate-buffered solutions (pH 7) at a concentration of approximately 200 μg/mL. A cuvette with

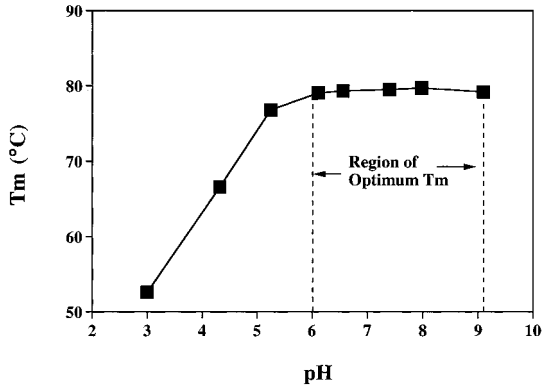

FIGURE 1: Plot of rhFlt3L T_m as a function of pH showing the region from pH 6 to 9 (bracketed by vertical dashed lines) where the T_m reaches a plateau. This pH region is of special interest for evaluating the impact of reversibility. An exothermic response due to aggregation obscured measurement of the T_m at pH 10.

a 0.1 cm path length was used in both cases. Scans were acquired at 1 nm step resolution from 260 to 190 nm at a speed of 10 nm/min. Sensitivity, in each case, was 20 mdeg with a time constant of 1 s. Nine scans were accumulated to improve the signal-to-noise ratio. The secondary structure estimates were determined by deconvoluting the spectrum into five structure elements by convex constraint analysis (CCA) as described previously (*16*, *17*).

WWF7 Bioassay. Bioactivity was measured with the WWF7 cell line (a murine Pro B-derived line) to detect the presence of active rhFlt3L (*18*). These cells were dependent upon rhFlt3L for long-term growth. Therefore, the addition of rhFlt3L stimulated the proliferation of the WWF7 cells in a dose-responsive manner, permitting quantitative determination in comparison to a reference standard of known activity. The amount of cell proliferation was measured by "pulsing" with tritiated thymidine. Incorporation of thymidine into DNA during cell division is the basis of the activity assessment. The amount of tritiated thymidine incorporation was detected with a direct β counter (counts per minute, cpm) for each sample and was directly proportional to the amount of WWF7 cell proliferation induced by rhFlt3L. The data are reported as a ratio of the specific activity for a given sample relative to that of a control (fully active rhFlt3L).

RESULTS

Optimal pH and T_m. Initial studies were intended to determine the pH optimum where the T_m achieved the highest temperature of unfolding since this had previously been shown to be an effective means to evaluate the stability of protein systems (*1*, *19*, *20*). A plot showing the behavior of the T_m as a function of pH is provided in Figure 1. The T_m of rhFlt3L exhibits a broad pH range extending from pH 6 to 9 where it essentially plateaus near 80 °C. On the basis of similar studies conducted on rhM-CSF (*1*) and knowing that it is a structurally related protein system (*9*), the region from pH 7 to 8 was suspected to be optimal for rhFlt3L stability. At pH 10, aggregation of the protein (indicated by an exotherm in the DSC measurement) obscured determination of the T_m and, therefore, precluded reporting T_m measurements at this pH and beyond.

The thermodynamic parameters of the microcalorimetry experiment showed that as pH was decreased from 7 to 6,

Table 1: Thermodynamic Parameters of Flt3 Ligand Unfolding

pH	ΔH_1 (kcal/mol)	ΔH_v (kcal/mol)	$\Delta H_1/\Delta H_v$	T_m (°C)
3.0	56.8	70.0	0.81	50.2
4.0	77.3	107.3	0.72	66.6
4.3	77.0	107.9	0.71	66.8
5.3	89.7	120.6	0.74	76.8
6.1	98.9	120.6	0.82	78.6
7.0	115.7	120.8	0.96	78.5
7.2	106.9	117.7	0.91	80.0
7.4	114.9	120.4	0.95	79.4

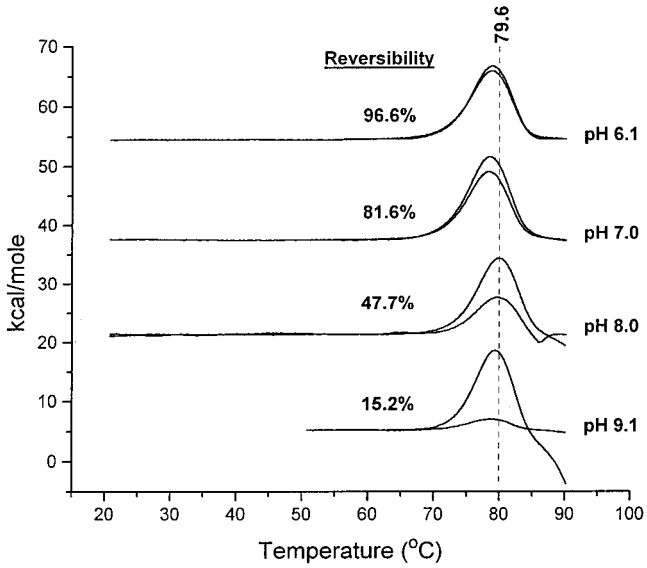

FIGURE 2: Concentration-normalized DSC scans showing the thermal reversibility behavior (determined by eq 1) of rhFlt3L across the pH range from pH 6.1 to 9.1. Heating to 90 °C was arbitrarily chosen to encompass the entire unfolding transition.

the calorimetric enthalpy of the first scan (ΔH_1) drops to lower values (Table 1). The accurate assessment of thermodynamic parameters at pH 8 and above was not included due to the difficulties associated with baseline changes related to the aggregation phenomena. However, knowing that pH 8 and 9 are within the region of the T_m plateau, it was plausible to assume that the enthalpy at these conditions was close to that observed from pH 6 to 7.4. Furthermore, the calorimetric to van't Hoff enthalpy ratio ($\Delta H_1/\Delta H_v$) approximates a two-state process between pH 6 and 7.4 with values close to unity. When the data from pH 6.1 to 7.4 were taken into account, the average enthalpy was 109.1 $\pm$ 7.9 kcal/mol. It was assumed that the two-state model could be applied throughout the region of the T_m plateau. Below pH 6 both the T_m and the enthalpy diminished (Table 1 and Figure 1).

Thermal Reversibility and Aggregation. Recombinant human Flt3L thermal reversibility within the pH region of the T_m plateau (pH 6−9) exhibited a contrasting trend that was suspected to confer stability in regard to the aggregation phenomenon. Since there was little change in T_m in this pH regime, it was possible to evaluate the effect of thermal reversibility independent of T_m and assess its importance on stability. Figure 2 illustrates this behavior showing the normalized enthalpy of the first and second scans with the accompanying reversibility at each pH tested. There was a progressive decrease in reversibility moving from pH 6 to 9. Hence, the succeeding investigation was undertaken to

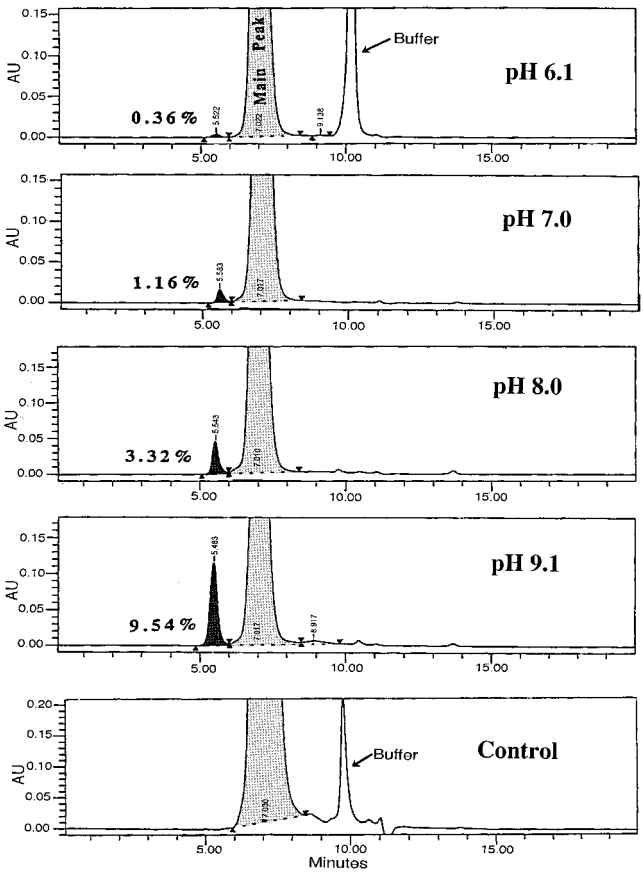

FIGURE 3: SEC of rhFlt3L samples incubated at 50 °C for 2 weeks. From top to bottom, studies were carried out at pH 6.1 (citrate-buffered), 7.0 (phosphate-buffered), 8.0 (phosphate-buffered), and 9.1 (phosphate-buffered). The control (Tris-buffered, pH 7.4) was freshly thawed protein that had been stored at −70 °C. The amount of aggregate (dark shaded band preceding the main peak) is expressed as a percentage of the combined main peak and aggregate band areas.

ascertain the importance of thermal reversibility in determining the best solution conditions for stabilizing rhFlt3L.

Continuing further with the notion that thermal reversibility could be used as a predictive parameter of stability for rhFlt3L, an accelerated study was carried out at 50 °C (well below the thermal unfolding and incipient melting of this protein). Solutions were examined after 2 weeks and 1 month. The SEC results at 2 weeks distinctly showed a progressive increase in the amount of aggregate species as denoted by the appearance of the eluting peak near 5.5 min (Figure 3). In fact, the progressive increase in aggregate seemed to follow the trend predicted by the thermal reversibility data obtained from the DSC measurements. The protein buffered at pH 6.1 (showing the highest thermal reversibility) was least prone to aggregate at 50 °C over a 2-week period. The relationship between thermal reversibility and aggregation (measured as a relative percent area) is illustrated in Figure 4. These data not only provide compelling evidence that unfolding of rhFlt3L is correlated to aggregation but also suggest that this process may be kinetically governed by the pH condition tested.

Nonreduced SDS−PAGE. The nonreduced SDS−PAGE data show signs of aggregation (high molecular weight bands and smearing labeled A and B) predominantly above pH 6 and the appearance of more breakdown below pH 6 (bands labeled E) (Figure 5). The negative staining associated with

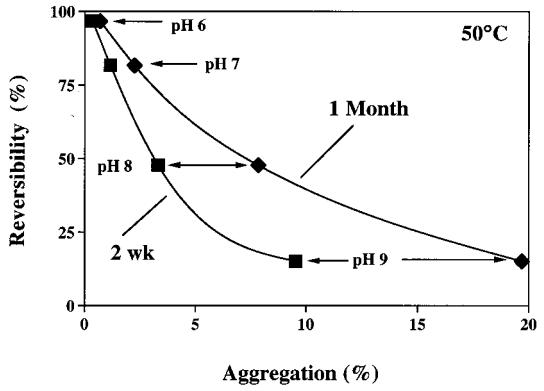

FIGURE 4: Plot depicting the relationship between thermal reversibility and protein stability as measured by the amount of rhFlt3L aggregation, defined by SEC at 2 weeks (■) and 1 month (◆) incubated at 50 °C and at designated pH.

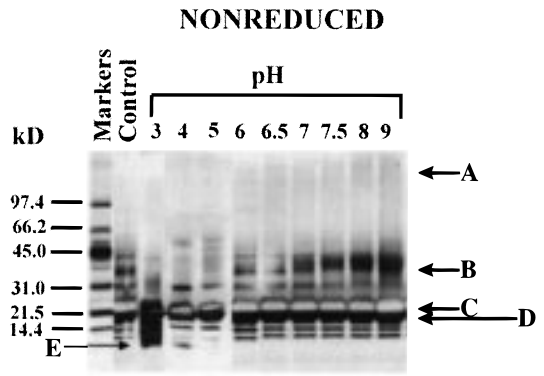

FIGURE 5: Nonreduced silver-stained SDS−PAGE of rhFlt3L incubated for 2 weeks at 50 °C. Data show large aggregate band smearing (A), intermediate aggregate (B), monomeric protein bands (C and D), and breakdown (E).

the C band on the gel is characteristic of a highly glycosylated form of the rhFlt3L molecule giving rise to a higher than 17.4 kDa molecular mass. The lower band designated at D is more in line with the expected molecular weight of the monomer. The least amount of aggregation was observed at pH 6.

rhFlt3L Native and Aggregate Characterization. In solution, the rhFlt3L molecule exists as a dimer as measured by the "three detector" method (Figure 6A) and confirmed by sedimentation velocity experiments (data not shown). The aggregate elutes much earlier than the native rhFlt3L dimer and, therefore, made it possible to adequately isolate it in pure form (Figure 6B). By use of CCA it was possible to estimate the secondary structure of both the native dimer and the pure aggregate. The CD data clearly show that a dramatic change in structure accompanies the formation of aggregate (Figure 7). Quantitative assessment of the differences in secondary structure between the native and aggregate forms is suggestive of unfolding that requires a substantial loss of helix. From convex constraint analysis, an estimated loss in α-helix of 28% (44% native α-helix − 16% denatured α-helix) and a concomitant increase in β-sheet by 31.9% (37.6 denatured β-sheet − 5.7% native β-sheet) predominate the aggregate protein structure. The loss in helix is almost completely accounted for in the formation of sheet.

WWF7 Bioactivity. The subsequent evaluation of the bioactivity distinctly showed an optimum at pH 6 after 2

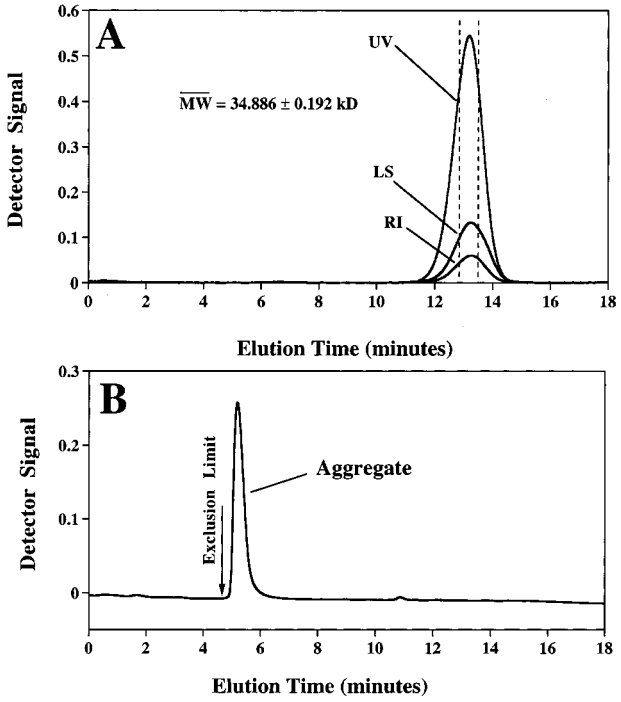

FIGURE 6: Molecular weight assessment of native rhFlt3L as determined by the "three detector" method (SEC−UV/LS/RI) is shown in panel A with designated detector signals labeled. The region bounded by the vertical dashed lines of the native eluting peak near 13 min represent 23 chromatographic slices used in the determination of the molecular weight with associated precision (±SD). Panel B displays the chromatogram of pure isolated aggregate reexamined by SEC showing that it is free of native protein. The aggregate species shown in panel B was obtained from a sample incubated for approximately 1 year at 50 °C near pH 9.

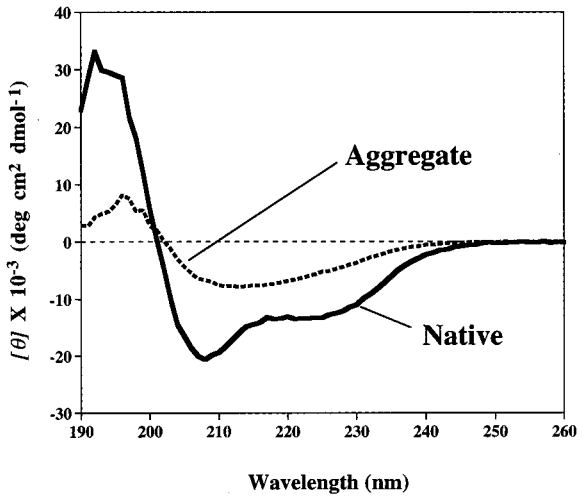

FIGURE 7: Far-UV CD spectra showing a dramatic difference in aggregate (dashed contour) and native (solid contour) rhFlt3L structure. By convex analysis, the secondary structure of the native state comprises about 44% α-helix, 6% β-sheet, 11% unordered, and 39% other structure. Analogously, the soluble aggregate is made up of 16% α-helix, 38% β-sheet, 17% unordered, and 29% other structure.

weeks at 50 °C (Figure 8). These results imply that aggregation had an effect on bioactivity and, thus, affected the efficacy of the protein. Aggregation is also known to elicit undesirable immunogenic responses (*21*). Again, these data follow the DSC reversibility assessment, providing additional evidence that thermal reversibility is an important parameter for defining stability of rhFlt3L in the pH region

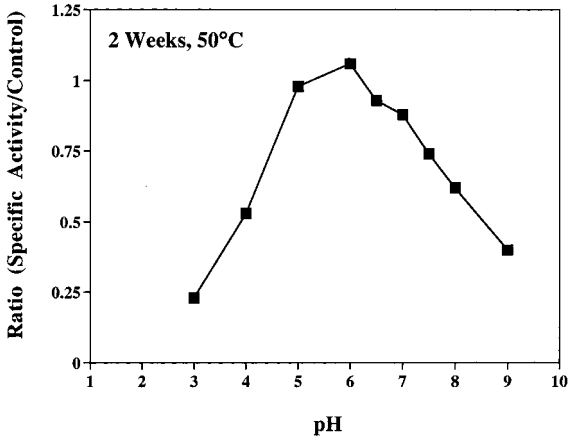

FIGURE 8: Bioactivity data taken as a ratio of the specific activity relative to that measure by a control plotted as a function of pH.

of optimal T_m. Knowing that the differences in T_m spanning from pH 6 to 9 are small and given that the T_m optimum does not align with the trend in minimizing aggregation, the reversibility was depicted as a more important parameter to assess stability. Yet, this does not discount the fact that this behavior was occurring at an essentially optimal T_m where conformational stability is expected to be the highest. Presented another way, solution conditions that favor the native state (conformational stability) and minimize interprotein interactions once unfolded should lower the susceptibility to aggregation. The results presented would suggest that both factors should be considered in the development of stable protein formulations.

DISCUSSION

Significance of Thermal Reversibility at the T_m Plateau. Other protein systems have been reported showing the same type of T_m plateau behavior as a function of pH. Such is the case for α-lactalbumin (22) and rhM-CSF (*1*). In general, the T_m of thermal unfolding for a given protein has been used as an index of protein stability (*1*, *2*, *20*). That is to say that a high T_m suggests high conformational stability. Yet little attention has been given to the role that thermal reversibility might play in these systems as an additional parameter for characterizing protein stability. In the protein cases mentioned, where the T_m achieves its highest point and remains essentially unchanged over a broad range of pH conditions, it can be difficult to discern which solution environment is important and offers the best potential for long-term stability.

In this study, the results clearly showed a correlation between thermal reversibility and aggregation. Within the plateau region, aggregation of rhFlt3L can be envisaged as a simple two-state unfolding model where thermal unfolding is a quasireversible process involving the native (N), denatured (D), and irreversibly denatured or aggregate (D_I) states.

$$N \underset{k_{-1}}{\overset{k_1}{\rightleftharpoons}} D \xrightarrow{k_2} D_I$$

In this model, the native state, referred to as the folded state, is in dynamic equilibrium with the denatured (or unfolded) state. Associated with the two-state equilibrium and formation of aggregate are the corresponding rate constants (k_1,

k_{-1}, and k_2). Between pH 6 and 7 (where the unfolding approximates a two-state process), the change in T_m with respect to pH is insignificant and therefore would suggest that the equilibrium between the N and D states is essentially unchanged. With this in mind, one can assume that the rate of D_I formation at a given pH is due to the change in the rate constant k_2. Hence, the rate-limiting irreversible step that leads to aggregate formation (governed by k_2) must be influenced by pH. This being the case, the pH dependence of the aggregate species is likely to be a reflection of an electrostatically dependent process (*23*). Additionally, unfolding of rhFlt3L is coupled to the aggregation process as evidenced by the significant alteration in secondary structure of the aggregate form (CD data of Figure 7). The results support a thermodynamic unfolding mechanism that competes with a kinetically driven aggregation process where the rate is augmented presumably by a change in protein net charge (i.e., rate dependence on the pH). Hence, the simple scheme above adequately explains how the thermal reversibility data measured in the DSC could account for the results at 50 °C for the different pH conditions spanning the plateau region.

Scan Rate and Concentration Factors in the Unfolding Region. In lieu of the thermal reversibility changes observed in the DSC scans across the T_m plateau (Figure 2), one could argue that the rate of aggregation is not fast enough in comparison to the scan rate during thermal unfolding to cause a shift in the equilibrium toward the denatured state. If indeed this was the case, a significantly lower T_m would be expected at conditions beyond pH 6 and approaching pH 9 where aggregation becomes more pronounced. Even at a slower scan rate of 60 °C/h there was no significant lowering in the T_m (data not shown). Additionally, evaluating protein concentration factors on aggregation from 14 to 1.3 mg/mL exhibited little change in the T_m (78.2 to 78.7 °C, respectively and 60 °C/h at pH 7.5). Hence, one would conclude that the aggregation rate is not fast enough relative to the scan rate between pH 6 and 9 and independent of protein concentration.

Two-State Mechanism and Inference to Unfolding Behavior. The current view of protein unfolding suggests that the native and subsequent intermediate (partially folded) states comprise an ensemble of substates possessing a core of nativelike structure (*24*, *25*). At solution conditions below pH 6, there was a tendency for the $\Delta H_l/\Delta H_v$ ratio to decrease somewhat, becoming less than unity (Table 1). Such behavior is presumably due to the prominence of intermolecular association during the unfolding process (*26*). What is interesting, however, is that $\Delta H_1/\Delta H_v$ values less than unity persist near pH 6 (at the edge of the T_m plateau). At higher pH conditions within the T_m plateau, the van't Hoff relation approaches unity, suggesting that intermolecular influences with respect to unfolding are weakened and that the unfolding behavior is essentially two-state (*27*). Hence, the ambiguity assuming an ensemble of substates where unfolding may be represented by a two-state model can be reconciled by assuming that the intermediate states make up a minor portion of the native to denatured state equilibrium and thus may be ignored (*26*−*28*). Additionally, the CD data allude to a radical change in structure at pH conditions associated with the T_m plateau showing an appreciable quantity of helix is lost in the formation of the aggregate. This amounts to an estimated 30−40% loss in native structure, suggesting that 60−70% nativelike structure remains.

It is intriguing to ponder how unfolding proceeds at temperatures well below the incipient melting point of the unfolding endotherm as was the case for the 50 °C studies. Although it could not be established whether unfolding at such temperature conditions proceeds as a gradual expansion arising from the loosening of the intramolecular hydrogen bonds (*29*, *30*) or simply as an all-or-none unfolding event governed by thermodynamics (*31*), it was clear that extensive unfolding occurred. In the present study, aggregate formation as described by the CD data exhibited an appreciable secondary structure change. The results suggest that the unfolded state involved a significant depletion of α-helix that is almost exactly offset by an increase of β-sheet in the formation of the aggregate. Additionally, net protein charge must also be important, since the aggregation phenomenon is exacerbated at increasing pH conditions above the p*I*. Globular proteins in general have compact configurations that are impenetrable by water near their isoelectric points (*31*). Since the T_m exhibits little change at pH conditions within the plateau region, it follows that the native state of rhFlt3L undergoes little configurational change as net negative charge is increased above the p*I*. With this knowledge, the combination of net protein charge and unfolding must be involved in the aggregation process. This interpretation of the data is consistent with the DSC results that also did not indicate any measurable evidence of stable intermediates at pH conditions associated with the T_m plateau.

Implications to Long-Term Stability. There are a number of instances where the irreversible behavior of thermal unfolding was attributed to aggregation (*32*−*34*). However, in modeling such responses, little emphasis has been placed on how thermal reversibility data might be used to address appropriate solution conditions to store and stabilize proteins. In the case of rhFlt3L, a correlation exists involving thermal reversibility and aggregation at 50 °C that connect protein unfolding/refolding with storage stability. Knowing that it is possible to predict and rank stability on the basis of the thermal reversibility outcome provides a means to decipher solution conditions that offer the best chances of long-term stability (as it pertains to the minimization of aggregation at the T_m plateau). Moreover, these data suggest that reliance on the T_m alone for predicting the best long-term stability conditions [as has been demonstrated for rhM-CSF (*1*) and IL-1R (*20*)] is inadequate in the case of rhFlt3L.

It has already been mentioned that the unfolding of rhFlt3L can be treated as a two-state mechanism within the region of the T_m plateau as suggested by the $\Delta H_1/\Delta H_v$ ratio (close to unity, Table 1). Knowing that the T_m is a measure of conformational stability, the plateau region would mark the pH conditions most appropriate for maintaining a stable compact structure (since it is inferred from the equilibrium to favor the native state). The change in the thermal reversibility across this region signifies the propensity of the unfolded state to aggregate. On this basis one might conclude that unfolding is the only prerequisite for the aggregation process. However plausible that might sound, it does not take into account the implications of pH change. Obviously, since rhFlt3L is above its p*I* in the plateau region, it is experiencing more net negative charge with the progression from pH 6 to 9. This would argue in favor of an additional prerequisite

involving the deprotonation of a residue or residues within this pH regime. Long-term stability, therefore, depends both on keeping the molecule conformationally stable and on maintaining a solution environment where deprotonation of ionized residues is minimized.

Optimal Stabilizing Conditions at the T_m Plateau. Finally, in examining the aggregation response between pH 6 and 9, the preferred solution condition associated with minimal aggregation was found to be near pH 6. This was confirmed by the SEC and SDS−PAGE data. The WWF7 data showed the greatest bioactivity to occur at pH 6. Not all protein systems are fully active at the conditions associated with high reversibility. Horse cytochrome *c*, for example, exhibits high thermal reversibility at acid pH conditions where the folded conformation of the protein is no longer fully active (*35*). Hence, it is not always possible to associate high thermal reversibilty with protein functionality. In some cases the net charge of the protein molecule (that is pH-dependent) may need to be taken into account with regard to biological activity (*36*). In the case of rhFlt3L, high thermal reversibility does correspond to the greatest bioactivity and stability. The combined SDS−PAGE, SEC, and bioactivity data suggest that it is important that rhFlt3L be conformationally stable and that solution conditions be adjusted so that susceptibility to aggregation is minimized once unfolded. This was accomplished with regard to achieving the highest thermal reversibility at the T_m plateau.

CONCLUSIONS

The preceding results and discussion provide evidence that thermal reversibility as measured by microcalorimetry can be an important parameter of stability in some protein systems. The corroborating evidence obtained from SEC, SDS−PAGE, and bioactivity clearly support this assessment for rhFlt3L. Additionally, reliance on the T_m alone was insufficient to correctly determine optimal stability conditions. However, knowing that these studies were conducted at conditions where the T_m was optimal, it seemed appropriate that the combination of high T_m (an indication that the native state is favored in the equilibrium step) and thermal reversibility (a measure of the susceptibility of the protein to aggregate once unfolded) are important for defining solution conditions where rhFlt3L aggregation is minimized. Secondary structure assessment of the aggregate species formed suggests that it proceeds from the unfolded state of the protein. Susceptibility to aggregation once unfolded is augmented with increasing pH within the plateau region.

ACKNOWLEDGMENT

We are grateful for the helpful assistance of Tenzin Gyaltsen in preparing some of the figures in the manuscript. Additionally, manuscript editing assistance from Anne Aumell was greatly appreciated.

REFERENCES

1. Schrier, J. A., Kenley, R. A., Williams, R., Corcoran, R. J., Kim, Y., Northey, R. P., Jr., D'Augusta, D., and Huberty, M. (1993) *Pharm. Res. 10*, 933−944.
2. Santoro, M. M., Liu, Y., Khan, S. M. A., Hou, L.-X., and Bolen, D. W. (1992) *Biochemistry 31*, 5278−5283.
3. Alexander, P., Fahnestock, S., Lee, T., Orban, J., and Bryan, P. (1992) *Biochemistry 31*, 3597−3603.
4. Pace, C. N., Shirley, B. A., Mcnutt, M., and Gajiwala, K. (1996) *FASEB J. 10*, 75−83.
5. Sturtevant, J. M. (1987) *Annu. Rev. Phys. Chem. 38*, 463−488.
6. Edge, V., Allewell, N. M., and Sturtevant, J. M. (1985) *Biochemistry 24*, 5899−5906.
7. Steadman, B. L., Trautman, P. A., Lawson, E. Q., Raymond, M. J., Mood, D. A., Thomson, J. A., and Middaugh, C. R. (1989) *Biochemistry 28*, 9653−9658.
8. Davio, S. R., Kienle, K. M., and Collins, B. E. (1995) *Pharm. Res. 12*, 642−648.
9. Lyman, S. D., and Jacobsen, S. E. W. (1998) *Blood 91*, 1101−1134.
10. Rozwarski, D. A., Gronenborn, A. M., Clore, G. M., Bazan, J. F., Bohm, A., Wlodawer, A., Hatada, M., and Karplus, P. A. (1994) *Structure 2*, 159−173.
11. Taylor, E. W., Fear, A. L., Bohm, A., Kim, S.-H., and Koths, K. (1994) *J. Biol. Chem. 269*, 31171−31177.
12. Wyatt, P. J. (1993) *Anal. Chim. Acta 272*, 1−40.
13. Arakawa, T., Langley, K. E., Kameyama, K., and Takagi, T. (1992) *Anal. Biochem. 203*, 53−57.
14. Wen, J., Arakawa, T., and Philo, J. S. (1996) *Anal. Biochem. 240*, 155−166.
15. Wen, J., Arakawa, T., Talvenheimo, J., Welcher, A. A., Horan, T., Kita, Y., Tseng, J., Nicolson, M., and Philo, J. S. (1996) in *Techniques in Protein Chemistry VII* (Marshak, D. R., Ed.) pp 23−31, Academic Press, Inc., New York.
16. Perczel, A., Hollósi, M., Tusnády, G., and Fasman, G. D. (1991) *Protein Eng. 4*, 669−679.
17. Perczel, A., Park, K., and Fasman, G. D. (1992) *Anal. Biochem. 203*, 83−93.
18. Brasel, K., Escobar, S., Anderberg, R., de Vries, P., Gruss, H.-J., and Lyman, S. D. (1995) *Leukemia 9*, 1212−1218.
19. Malakauskas, S. M., and Mayo, S. L. (1998) *Nat. Struct. Biol. 5*, 470−475.
20. Remmele, R. L., Jr., Nightlinger, N. S., Srinivasan, S., and Gombotz, W. R. (1998) *Pharm. Res. 15*, 200−208.
21. Moore, W. V., and Leppert, P. (1980) *J. Clin. Endocrinol. Metab. 51*, 691−697.
22. Griko, Y. V., Freire, E., and Privalov, P. L. (1994) *Biochemistry 33*, 1889−1899.
23. Dill, K. A. (1990) *Biochemistry 29*, 7133−7155.
24. Chen, H. M., You, J. L., Markin, V. S., and Tsong, T. Y. (1991) *J. Mol. Biol. 220*, 771−778.
25. Uversky, V. N., Karnoup, A. S., Segel, D. J., Seshadri, S., Doniach, S., and Fink, A. L. (1998) *J. Mol. Biol. 278*, 879−894.
26. Privalov, P. L., and Potekhin, S. A. (1986) *Methods Enzymol. 131*, 4−51.
27. Mücke, M., and Schmid, F. X. (1994) *Biochemistry 33*, 12930−12935.
28. Makhatadze, G. I., Clore, G. M., Gronenborn, A. M., and Privalov, P. L. (1994) *Biochemistry 33*, 9327−9332.
29. Frushour, B. G., and Koenig, J. L. (1975) in *Advances in Infrared and Raman Spectroscopy* (Clark, R. J. H., and Hester, R. E., Eds.) pp 35−97, Heyden & Sons Ltd., New York.
30. Maneri, L. R. (1990) *Biochem. Biophys. Res. Commun. 166*, 1365−1371.
31. Tanford, C. (1961) *Physical Chemistry of Macromolecules*, pp 515−521, John Wiley & Sons, Inc., New York.
32. Chan, H.-K., Au−Yeung, K.-L., and Gonda, I. (1996) *Pharm. Res. 13*, 756−761.
33. Martínez, J. C., Harrous, M. E., Filimonov, V. V., Mateo, P. L., and Fersht, A. R. (1994) *Biochemistry 33*, 3919−3926.
34. Kono, M., Sen, A. C., and Chakrabarti, B. (1990) *Biochemistry 29*, 464−470.
35. Liggins, J. R., Sherman, F., Mathews, A. J., and Nall, B. T. (1994) *Biochemistry 33*, 9209−9219.
36. Davis, S. J., Davies, E. A., Tucknott, M. G., Jones, E. Y., and van der Merwe, P. A. (1998) *Proc. Natl. Acad. Sci. U.S.A. 95*, 5490−5494.

BI982881G